Nox1 Induces Differentiation Resistance in Immortalized Human Keratinocytes Generating Cells that Express Simple Epithelial Keratins

Walee Chamulitrat[1], Axel Huber[1], Hans-Dieter Riedel[1] and Wolfgang Stremmel[1]

We have shown that superoxide radical-generating NADPH oxidase 1 (Nox1) is increased in intermediate human transformed cells. It was unknown whether Nox1 overexpression could accelerate early transformation steps. We demonstrated that Nox1 rendered human immortalized (GM16) keratinocytes resistant against Ca^{2+}/serum-induced differentiation. Nox1-transfected cells produced fast dividing resistant cells within 7–10 days after DMEM exposure. Progenitor lines (or Nox1 lines) were reproducibly generated from Nox1-transfected cells, while no lines were obtained from control transfections. From several attempts to generate control cells, one resistant population was obtained from untransfected GM16 cells after a 6-week DMEM exposure. Prolonged passaging of the control line could induce Nox1. Compared with the control line, Nox1 lines showed greater expression of Nox1, Rac1, p47*phox*, p67*phox*, NOXO1, and NOXA1 with concomitant increased superoxide generation. All five Nox1 lines contained varying amounts of E-cadherin, involucrin, vimentin, and K8/K18, while the control line did not. Since vimentin and K8/K18 are associated with malignant progression in different types of human epithelial tumors, our data demonstrate that Nox1 accelerated neoplastic-like progression by inducing generation of progenitor cells. Our data also emphasize the importance of Nox1 in inducing resistance against differentiation-induced cell death, suggesting a contribution of Nox1 and its oxidants during early stage of cell transformation.

Journal of Investigative Dermatology (2007) **127,** 2171–2183; doi:10.1038/sj.jid.5700843; published online 26 April 2007

INTRODUCTION

Reactive oxygen species (ROS) including superoxide radical and hydrogen peroxide produced by cancer cells are involved in neoplastic transformation and progression (Gupta *et al.*, 1999). Some of the sources of ROS are NAD(P)H oxidase homologs NADPH oxidase 1 (Nox1)–Nox5 (Cheng *et al.*, 2001). Nox1 was first described to mediate tumorigenic conversion of mouse fibroblasts (Suh *et al.*, 1999). For human keratinocytes, overexpression of Nox1 increases tumorigenic potentials of the prostate cancer cell line (Arbiser *et al.*, 2002). Nox1 is present in human prostate cancer (Lim *et al.*, 2005), colon tumors (Geiszt *et al.*, 2003), and adenoma, and well-differentiated adenocarcinoma of human colon (Fukuyama *et al.*, 2005). Thus, Nox1 is associated with late-stage epithelial malignancies. It is not known whether Nox1 has any influence on an early transformation stage of human keratinocytes, particularly, regarding overcoming of differentiation-induced cell death with subsequent acquisition of indefinite lifespan.

Functional studies in the nonmalignant human immortalized HaCaT cell line have revealed the presence of Nox and its activation by growth factors (Goldman *et al.*, 1998) or Ras (Yang *et al.*, 1999). We reported that one of the HaCaT Nox isoforms was Nox1 (Chamulitrat *et al.*, 2004). In model nonmalignant immortal cells we had previously developed (Chamulitrat *et al.*, 2003a), the less transformed EPI cells expressed low levels of Nox1, whereas more transformed FIB cells expressed increased Nox1 (Chamulitrat *et al.*, 2003b). Unlike primary human keratinocytes, HaCaT, EPI, and FIB cells proliferate well in standard DMEM, which contains high Ca^{2+} levels. This raises the possibility of whether Nox1 expression might confer resistance against differentiation induced by high Ca^{2+} present in DMEM and serum. In multistep carcinogenesis, resistance against terminal differentiation is regarded as a criterion for selecting preneoplastic keratinocytes (Rheinwald and Beckett, 1980; Kulesz-Martin *et al.*, 1983). Such selection has been described during inhibition of terminal differentiation upon transfection of an oncogene such as Ras (Kulesz-Martin *et al.*, 1983), HPV16 E6 (Sherman and Schlegel, 1996), or treatment with 12-*o*-tetradecanoylphorbol-13-acetate (Karen *et al.*, 1999). Furthermore, it has been shown that resistance

[1]*Department of Internal Medicine IV, University of Heidelberg, Heidelberg, Germany*

Correspondence: Dr Walee Chamulitrat, Department of Internal Medicine IV, Forschungsgruppen, Im Neuenheimer Feld 345, 69120 Heidelberg, Germany. E-mail: Walee_Chamulitrat@med.uni-heidelberg.de

Abbreviations: AIG, anchorage-independent growth; DMEM/FCS, DMEM containing 10% FCS; FCS, fetal calf serum; IFs, intermediate filaments; IIF, indirect immunofluorescence; KGM, keratinocyte growth medium; Nox, NADPH oxidase; PD, population doubling; ROS, reactive oxygen species.

Received 9 August 2006; revised 3 January 2007; accepted 30 January 2007; published online 26 April 2007

against differentiation (or apoptosis) of human immortalized cells is enhanced by an additional stress such as benzo[*a*]pyrene (Yang *et al.*, 1992), asbestos fibers (Zhao *et al.*, 2000), or hypoxia (Kim *et al.*, 1997), and this corresponds to increased neoplastic progression.

Studies in rodent cells in culture have revealed that genetic alterations followed by selective clonal expansion lead to preneoplastic phenotype (Rubin, 2001). Epigenetic selection including culture conditions such as high-density prolonged cultures can increase neoplastic progression. Prolonged confluence allows genetic variants to emerge, multiply, and acquire transformation-related genetic changes under high-density cell culture conditions (Rubin, 2001). Prolonged confluent cultures have been used to select immortalized or preneoplastic human cells (Zhu and Gooderham, 2002; Goldring, 2004). Furthermore, repeated rounds of prolonged confluence culture induced conversion of NIH3T3 (Rubin 2001), and rat liver epithelial cells (Lee *et al.*, 1989) to malignancy. For the purpose of selecting Nox1-dependent preneoplastic cells, we adopted repeated rounds of confluent cultures to our experimental designs. We aimed to demonstrate that Nox1 accelerated resistance against Ca^{2+}/serum-induced differentiation in immortalized cells to generate cells with indefinite lifespans.

We performed Nox1 overexpression of human gingival mucosal keratinocytes immortalized by human papillomavirus type16 E6/E7 (GM16 cells), which normally proliferate in low-Ca^{2+} keratinocyte growth medium (KGM). After three to five rounds of confluence, GM16 cells transfected with Nox1 were resistant against high Ca^{2+} in DMEM and serum. Five Nox1 progenitor lines were obtained, whereas only one control line was obtained after several attempts. Compared with the control line, Nox1 lines showed greater expression of Nox-based components, with concomitant increased ROS generation. Our data provide novel evidence that Nox1 is involved in the selection of immortalized keratinocytes to produce progenitor cells that are in accelerated steps of cell transformation.

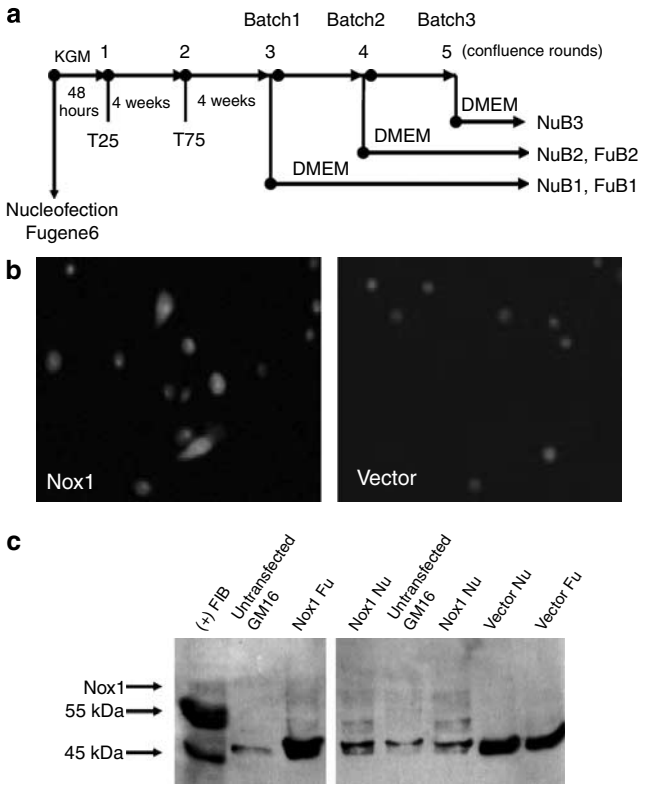

Figure 1. Experimental design for generation of Nox1 lines capable of proliferating in DMEM/FCS. (**a**) Scheme for generation of Nox1 lines from transfection of GM16 cells as described in Materials and Methods. After Nucleofection and Fugene6 transfections, cells were maintained at a stationary state for two rounds. Trypsinization at round 3 was designated as Batch1. Selection was carried out by exposing cells to DMEM/FCS without any trypsinization but with changes of DMEM/FCS. Resistant cells against Ca^{2+}/serum-induced differentiation were fast-dividing cells as shown in Figure 2a. (**b**) Generation of ROS during transient transfection (as shown for Nucleofection) of GM16 cells with pcDNA3.1/Nox1 (Nox1) or pcDNA3.1 (vector). Transfected cells were treated with 10 μM hydroethidine for 20 min at 37°C. After washing, cells were inspected under a fluorescence microscope. (**c**) Western blot analysis of Nox1 in membranes of transfected GM16 cells from $\sim 30 \times 10^6$ Batch1 cells. Membrane proteins of 10 μg were loaded in each lane. Our freshly prepared Nox1 antibody reacted strongly with 55- and 45-kDa proteins but weakly with Nox1 at 63 kDa. Membranes from FIB cells were used as (+) controls. In all samples, an unspecific crossreaction with a 45-kDa protein was observed.

RESULTS

Transfection of GM16 cells

The procedure to generate stable Nox1 lines as described in Materials and Methods is shown in Figure 1a. Similar to primary keratinocytes, GM16 cells are difficult to transfect and we therefore performed two types of transfections in parallel using Nucleofection technology and liposomal DNA delivery with Fugene6. Briefly, pcDNA3.1- or pcDNA3.1/Nox1-transfected GM16 cells underwent two rounds of confluence in G418-containing KGM for 4 weeks each round. At the third round, cells were exposed to DMEM containing 10% fetal calf serum (FCS) (DMEM/FCS) for selection, which was designated as Batch1. Same sequence was carried out for Batches 2 and 3. The obtained Nox1 lines were named according to transfection type and batch number as NuB1, FuB1, NuB2, FuB2, and NuB3. FuB3 cells did not proliferate and died.

To demonstrate that our Nox1 constructs were functional, we determined generation of ROS following transient transfection of GM16 cells by either Nucleofection or Fugene6. As shown in Figure 1b, pcDNA3.1/Nox1 transfection produced ROS-positive cells exhibiting strong red fluorescence of oxidized hydroethidine in the nucleus and cytoplasm. From a total of ~1,200 counted cells, Nox1 transfection by both types of transfection caused a two-fold increase of cells generating ROS (2.0–2.5% for vector pcDNA3.1 vs 4.4–5.3% for pcDNA3.1/Nox1). Non-transfected GM16 cells produced very small amounts of ROS-positive cells at ~0.5%, indicating that transfection caused increases in the number of ROS-positive cells to ~2%. Our Nox1 constructs were effective in increasing the number of ROS-positive cells to ~4–5%. This was much lower than the ~50% efficiency obtained from GFP-pmax transfection,

indicating our transfection with very low efficiency was likely due to the use of pcDNA3.1 and hydroethidine for probing ROS.

To generate stable Nox1 lines, we performed another set of transfections and carried out the procedure as outlined in Figure 1a. Transfected GM16 cells from Batch1 after three rounds of confluence (of a total $\sim 3 \times 10^6$ cells) were collected for Western blot analysis of Nox1 (Figure 1c). To produce our anti-Nox1 antibody, we used the same peptide sequence against C-terminus of human Nox1 as previously reported for Nox1C2 antibody (Kawahara *et al.*, 2004). For positive control, we used membranes from FIB cells previously shown to contain Nox1 (Chamulitrat *et al.*, 2003b), and our antibody detected a weak signal at 63 kDa and strong signals at 55 and 45 kDa (Figure 1c). When diluted, and the Nox1 antibody again reused, we found that the 55-kDa band became much weaker (Figure 3b). Owing to a small number of transfected Batch1 GM16 cells for membrane preparation, we could only observe two faint protein bands between 50 and 65 kDa in membranes of Nox1-Fugene6-transfected (Nox1 Fu) and -nucleofected (Nox1 Nu) GM16 cells. Membranes from untransfected parental or vector-transfected GM16 cells were immunoreactive only with a 45-kDa protein, indicating that this protein was likely from an unspecific reaction. The 45-kDa protein had previously been detected in HaCaT membranes using Nox1C2 antibody (Chamulitrat *et al.*, 2004). In Nox1-transfected GM16 cells and (+) FIB cells, Nox1 at 63 kDa appeared as a very faint band whereas the 55-kDa protein was clearer (Figure 1c). This unassigned 55-kDa protein was previously observed in cytosolic and nuclear fractions of EPI and FIB cells (Chamulitrat *et al.*, 2003b). A recent report (Hilenski *et al.*, 2004) has shown the presence of both 63- and 50-kDa proteins using their Nox1 antibody. At this time, we do not know the identity of the 55-kDa protein, but it appeared every time the 63-kDa Nox1 was detected. We plan to determine the amino-acid sequence of this 55-kDa protein in the future.

Induction of resistance against terminal differentiation by Nox1

Batch1-transfected GM16 cells were split for Nox1 protein analysis (shown in Figure 1c), for further subcultures to Batch2 and for selection in DMEM/FCS (Figure 1a). Upon DMEM/FCS exposure, differentiated cells stratified and died off, leaving empty spaces in cultures. For Nox1 transfections, resistant cells were first observed as small fast-dividing cells after DMEM/FCS exposure for 7–10 days. These cells transfected with Nox1 (named as Nox1 lines NuB1, FuB1, NuB2, FuB2, and NuB3) grew rapidly into empty spaces that differentiated cells had peeled off (Figure 2a). All vector-transfected cells (as shown for vector FuB1) did not produce these fast-dividing cells (Figure 2a). For Nox1 lines, the first appearance to the first trypsinization to passage 1 (p1) took ~3 weeks for Batch1, and increased to 6–10 weeks for Batches2 and 3, respectively. After trypsinization, all five Nox1 lines readhered and proliferated as shown for NuB1p2 and FuB1p2 in Figure 2b. The morphology of Nox1 NuB1 differed from four other Nox1 lines. NuB1 exhibited mixed morphology of enlarged cobblestone and spindle-shaped cells and the latter appeared to be less adhesive (indicated by an arrow in Figure 2b). Upon passaging, these cells gradually became homogeneously spindle-shaped and proliferated with slow growth rates. Four other Nox1 lines as shown for Nox1 FuB1p2 were cobblestone small cells with high proliferative capacity (Figure 2b). Vector transfection (either Nucleofection or Fugene6) initially produced spindle-shaped and flat cells, which had different extended-life cultures in DMEM/FCS. These cells subsequently lost proliferative capacity, resulting in no resistant cells as shown for vector FuB1p2 in Figure 2b.

We were unable to obtain any resistant cells from vector-transfected cells from all three batches. Virtually all vector-transfected cells had some limited lifespan; some could be passaged up to p14. Later they senesced and died off in DMEM/FCS. Furthermore, no persistent resistant cells were obtained in Nox1-transfected cells without undergoing rounds of confluence in KGM. After several attempts to obtain a control line from untransfected GM16 cells, only one population was obtained, but it maintained a very slow growth rate at $P<20$. These cells became proliferative at $P>20$ with the same growth rates as Nox1 lines (Table 1).

At ~30 passages, NuB1p31 was homogeneously spindle-shaped and four Nox1 lines as shown for FuB1p35 were cobblestone; control p34 was polygonal (Figure 2c). NuB1 and control cells grew as single cells rather than compact colonies. Nox1 lines with cobblestone morphology showed good uniform growth in DMEM/FCS with population doubling (PD) per day of ~0.4–0.5 (Table 1). This growth rate was the same as for parental GM16 cells cultured in KGM. The NuB1 line, however, had negative growth at early passages and these cells underwent a gradual change with increasing numbers of cells displaying better growth at p14 with PD per day of 0.5. Compared with NuB1, the control line had even slower growth rates with negative growth in the first 15 passages. Upon passaging, control cells, while maintaining their spindle-shapes, had an increasing number of cells with better growth reaching PD per day of 0.5 at $p>20$. None of the Nox1 or control lines at p20–32 exhibited any anchorage-independent growth (AIG), indicating that these cells were stable epithelial phenotypes that had not yet progressed to an advanced AIG stage.

Increased Nox1 expression and ROS generation by Nox1 lines compared with control

At first available passages, Nox1 and control lines were collected for Nox1 analysis using FIB membrane as (+) control (Figure 3a). In the FIB membrane, freshly diluted antibody detected Nox1 at 63 kDa as well as very strong 55- and 45-kDa bands in both unsolubilized and urea-solubilized membranes. Only a 45-kDa protein was detected in membranes of failed transfected (FT) cells at p5. The defined FT cells were GM16 cells Fugene6-transfected with pcDNA3.1/Nox1 and exposed to DMEM 48 hours later without going through rounds of confluence. FT-resistant cells were obtained after DMEM exposure for 10 weeks were proliferative for some time, and subsequently died off. Nox1

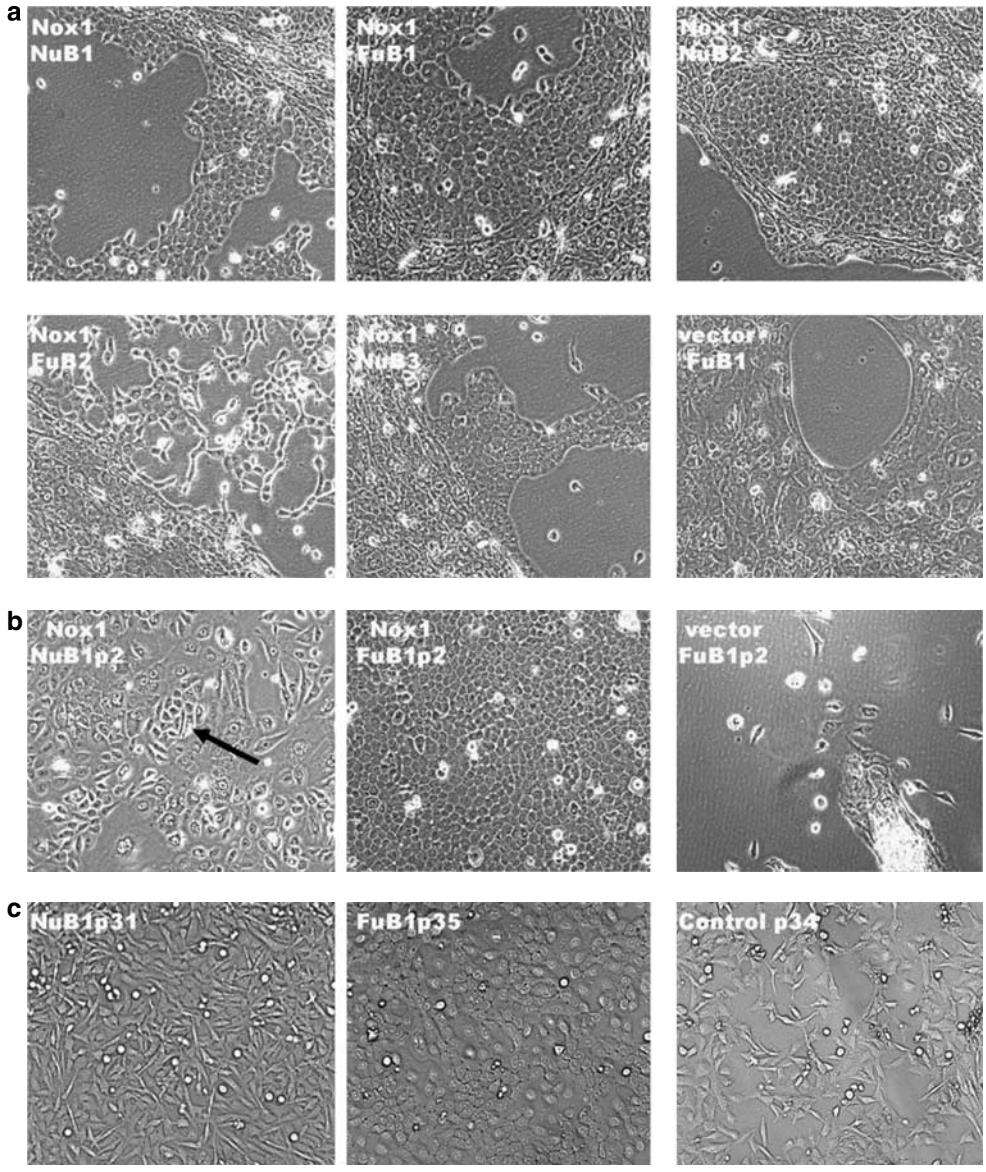

Figure 2. Morphological changes in GM16 cells following transfections and exposure to DMEM/FCS (Nu for Nucleofection and Fu for Fugene6). (**a**) Following exposure to DMEM/FCS for 7–10 days, resistant cells were observed as small fast-dividing cells from Nox1 transfection designated as Nox1 NuB1, FuB1, NuB2, FuB2, and NuB3. All vector-transfected cells were differentiated without formation of resistant cells as shown for vector FuB1. Resistant cells from Nox1 lines grew to confluence after 3–4 weeks in DMEM/FCS and were then passaged to p1. (**b**) At p2, Nox1 NuB1p2 cells were a mixture of cobblestone and spindle-shaped cells; the latter were less adhesive as indicated by an arrow. The other four Nox1 lines shown for Nox1 FuB1p2 were cobblestone exhibiting highly proliferative capacity. Vector-transfected cells as shown for vector FuB1p2 died off. (**c**) Phase-contrast micrographs at p > 30 show that NuB1p31 were fibroblast-like cells, while the other four Nox1 lines as shown for FuB1p35 were epithelium-like cells. Many attempts had been made to obtain control cells capable of growing in DMEM/FCS (described in Materials and Methods). Only one control line was obtained from untransfected GM16 cells after 6 weeks in DMEM/FCS. These cells had negative growth and later became proliferative (Table 1). Phase-contrast image of control p34 showed polygonal-shaped cells.

at 63 kDa and an unknown protein at 55 kDa were detected in the membranes of FuB1p20 and NuB2p7. Membranes of NuB1p10 (with negative growth, Table 1) showed almost undetectable 63-kDa Nox1 and weak 55-kDa protein. In urea-solubilized membranes, controls p4 and p10 (with negative growth, Table 1) showed an almost undetectable band, which appeared to be slightly lower than 63 kDa (Figure 3a).

We next measured Nox1 protein in control and Nox1 lines at later passages p > 30–40, which were all stable cells growing with similar PD (Table 1). Freshly prepared diluted antibody produced strong signals of 63, 55, and 45 proteins in all membranes, but the band of the control p41 membrane appeared to be slightly lower than 63 kDa, as marked with a dotted arrow (Figure 3b, left panel). When the diluted antibody was reused to incubate another blot of the same samples (except for (+) HaCaT), detection of 55 kDa was greatly reduced, indicating that the 55-kDa antibody had been removed from the first use (Figure 3b, right panel). Nox1 at 63 kDa was still detected in the NuB1p37, FuB1p42, and

Table 1. Growth characteristics of Nox1 and control lines cultured in DMEM/FCS, and parental GM16 cells in KGM

		PD per day[1]	Morphology
Parental GM16 cells in KGM			
GM16 p34 in KGM		0.40	Cobblestone
Nox1 lines in DMEM/FCS			
NuB1	p6	−0.008	Polygonal
	p14	0.54	Spindle-shaped
	p22	0.25	Spindle-shaped, patchy islands
FuB1	p14	0.40	Cobblestone
NuB2	p4	0.41	Cobblestone
	p18	0.47	
FuB2	p3	0.40	Cobblestone
NuB3	p2	0.56	Cobblestone
Control line in DMEM/FCS [2]			
GM16	p2	−0.10	Polygonal
	p15	−0.13	Polygonal
	p21	0.50	Polygonal

DMEM, Dulbecco's modified Eagle's medium; FCS, fetal calf serum; Nox1, NADPH oxidase 1.
[1]PD per day was calculated based on formular; PD=$\log_2$ (number of cells at the time of harvest)/(number of cells seeded) divided by number of days in culture. Each value was an average from 2–4 dishes.
[2]Control line was differentiation-resistant cells generated from untransfected GM16 cells (see Materials and Methods for details).

NuB2p30 membranes as compared with (+) FIB and HaCaT. Again, controls p41 and NuB1p37 showed another protein band which was slightly lower (~3 kDa) than Nox1 at 63 kDa (as marked with a dotted arrow). Under these conditions, Nox1 antibody apparently detected Nox1-specific protein(s) as a doublet. A doublet Nox1 was previously observed in (+) FIB2 (Figure 3a), rat smooth muscle cells (Lassegue *et al.*, 2001), Ras (+) NIH3T3 (Mitsushita *et al.*, 2004), and T84 (Kuwano *et al.*, 2006). The significance of this smaller size Nox1 is not known but appears to be Nox1-specific. Highly proliferative epithelium-like Nox1 lines (FuB1 and NuB2) in both low and high passages readily expressed 63-kDa Nox1 (Figure 3 a and b). NuB1 at high passages expressed detectable 63-kDa Nox1 and smaller-sized Nox1. In the control line, a strong doublet with smaller-sized Nox1 was detected only at high passages (Figure 3b), indicating that Nox1 may have been induced during passaging to generate stable phenotype.

To cooperate with Nox1 expression, ROS generation by Nox1 lines was compared with the control line. Dichlorofluorescein (DCF) fluorescence indicative of ROS generation was determined by FACS analysis (Figure 3c). NuB1p34, FuB1p38, and NuB2p26 showed increased DCF fluorescence compared with control p37, as observed with an FL1 shift to the right. From three different batches of cells, Nox1 lines produced more ROS by ~2–4-fold compared with the control line. An addition of EGF further increased ROS in all control and Nox1 lines. To measure superoxide radical generation specifically, an enhanced luminescence-based assay was utilized (Figure 3c). NuB1p41, FuB1p46, and NuB2p35 produced increased luminescence by ~2-fold compared with control p45. An addition of superoxide dismutase significantly inhibited luminescence in NuB2p35 indicating specificity for superoxide radical generation.

It has been shown that Nox1 requires small GTPase Rac1, organizer 1 (NOXO1), and activator 1 (NOXA1) for full activation of its superoxide-generating capacity (Kawahara *et al.*, 2004; Cheng *et al.*, 2006; Miyano *et al.*, 2006). In our study, Rac1 protein was expressed in NuB1p32, FuB1p36, and NuB2p24 at higher levels than in control p33 (Figure 3d). Rac1 protein was significantly increased upon passaging of control or NuB1 cells to their stable phenotypes. Nox1, p22*phox*, p47*phox*, p67*phox*, and NOXA1 mRNA were detected in all control and Nox1 lines. NOXO1 mRNA was detected only in NuB1p34 and (+) Caco-2 (Figure 3d).

Analysis of desmoplakins and E-cadherin in control and Nox1 lines

We investigated epithelial cell-to-cell adhesion proteins, which could be different among Nox1 and control lines. Similar to indirect immunofluorescence (IIF) of EPI cells (Chamulitrat *et al.*, 2003a), desmoplakins 1 and 2 were stained at interjunctional cell-to-cell contacts in FuB1p19 (Figure 4a, left panel) and NuB1p8 (not shown). Desmoplakins were, however, absent in control p6 (Figure 4a, right panel). Similar to EPI cells in DMEM/FCS and GM16 cells in KGM, all Nox1 lines as shown for FuB1p27 expressed high levels of E-cadherin as seen at cell-to-cell junctions (Figure 4b, left panel). NuB1p11 cells expressed weaker E-cadherin (not shown). A few control p11 cells were stained positive for E-cadherin (Figure 4b, right panel). Western blot analysis of control p9 and p33 consistently showed weaker and undetectable E-cadherin. E-cadherin was completely absent in NuB1p32, indicating loss of this protein upon passaging. For (+) and (−) controls, E-cadherin was present in epithelium-like EPI cells and absent in fibroblast-like FIB cells. Terminal differentiation marker involucrin was expressed at about the same levels in slow-growing control p9 or NuB1p11 and fast-growing FuB1p23 or NuB2p10 (Figure 4c). While NuB1p32, FuB1p36, and NuB2p24 retained involucrin expression, control p33 completely lacked involucrin, indicating that this line had impaired terminal differentiation. Cells lacking involucrin have previously been described as unusual strains of human keratinocytes (Adams and Watt, 1988). Our control cells may represent these ''non-differentiating'' keratinocytes.

Analysis of vimentin and simple epithelial keratin K8/K18

Intermediate filaments (IFs) constitute a diverse family of proteins according to their expression in specific cell types. Events such as differentiation resistance controlling differential expression of IF are involved in a process leading to transformation. Both NuB1 and control lines were elongated, suggesting alterations of cell-to-cell contacts in these cells in

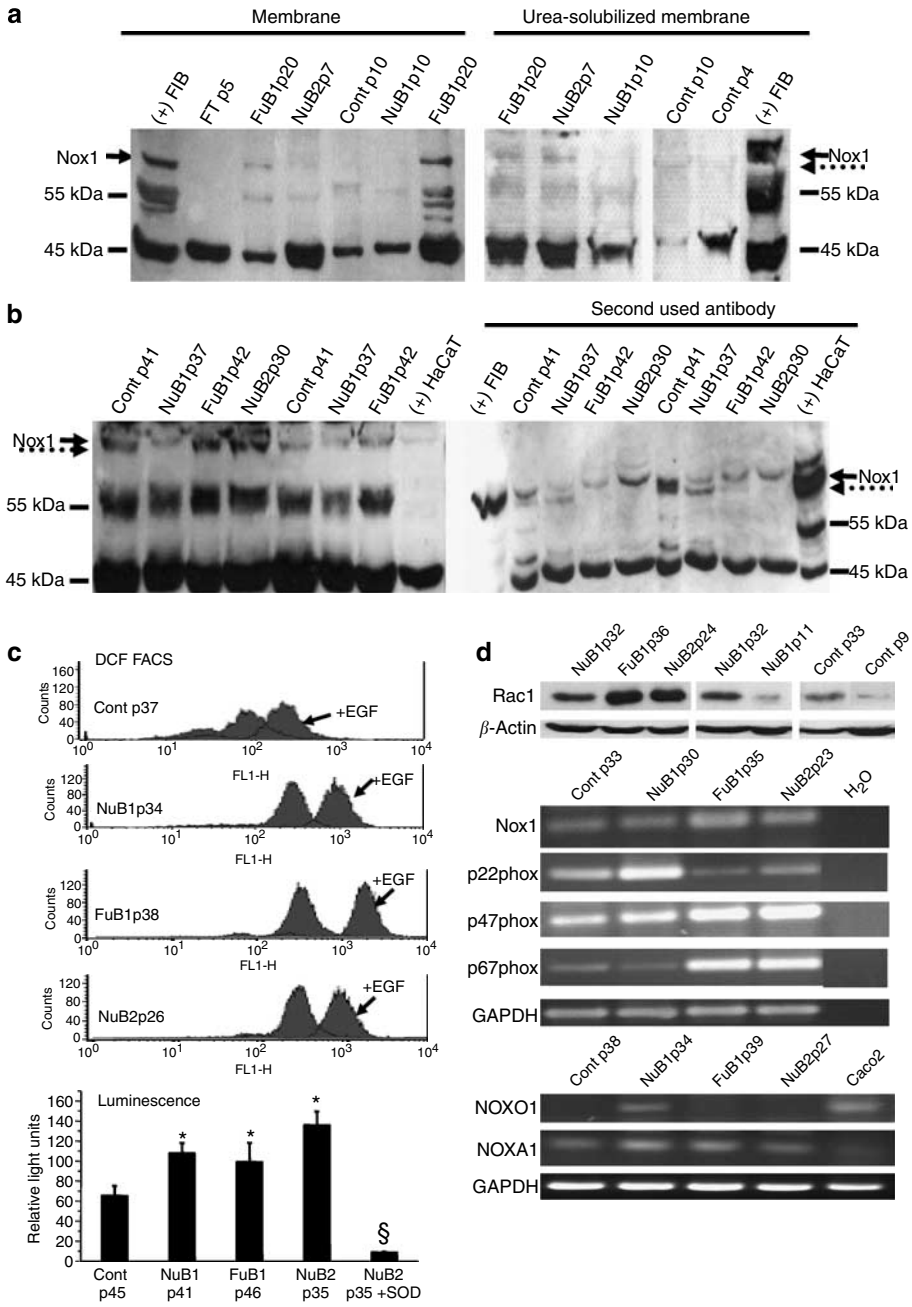

Figure 3. Expression of Nox1- and Nox-based components and ROS generation in Nox1 lines compared with control. (**a**) Western blot analysis of Nox1 lines in unsolubilized or urea-solubilized membrane of low passaged FuB1p20, NuB2p7, NuB1p10, and control p4 (50 μg each lane). FT (failed transfection) cells were resistant cells obtained from GM16 cells transfected with pcDNA3.1/Nox1 and exposed to DMEM/FCS for 10 weeks, and these cells lost proliferation and died at p14. FT cells, NuB1p10, and control p4 exhibited negative growth rates. Freshly prepared Nox1 antibody detected Nox1 at 63 kDa and strong proteins at 55 and 45 kDa in both membrane preparations. (**b**) Western blot analysis of Nox1 lines in membranes (50 μg each lane) of high passaged NuB1p37, FuB1p42, NuB2p30, and control p41 lines. Freshly prepared Nox1 antibody was used once, and 63-kDa Nox1 and strong 55- and 45-kDa proteins were detected (left panel). This diluted antibody was reused to incubate nitrocellulose membrane of another set of samples; 63-kDa Nox1 was readily detected in all samples while 55-kDa band was almost undetectable (right panel). Membranes (50 μg each) of FIB and HaCaT cells were used as (+) controls. Control p41 and NuB1p37 showed the presence of protein(s) at slightly lower than 63 kDa as indicated by a dotted arrow. (**c**) Oxidation of dichlorofluorescein diacetate to DCF by ROS generated by control and Nox1 lines was measured by FACS as green fluorescence (FL1). An addition of EGF (100 ng/ml) before dichlorofluorescein diacetate increased ROS in all cell types (top panel). Enhanced luminescence as an indicator of superoxide generation was determined in control and Nox1 lines (bottom panel). Superoxide dismutase (3 μg/ml) was used to inhibit luminescence of NuB2p35 (§ $P<0.05$ *vs* NuB2p35). Increased ROS were found in Nox1 lines (*$P<0.05$ *vs* control p45). (**d**) Rac1 protein was measured in 25 μg protein cell lysates. Nox1 lines expressed increased Rac1 protein compared with the control line. Nox1, p22*phox*, p47*phox*, p67*phox*, and NOXA1 mRNAs were present in all Nox1 and control lines. NOXO1 mRNA was detected in NuB1p34 and Caco-2.

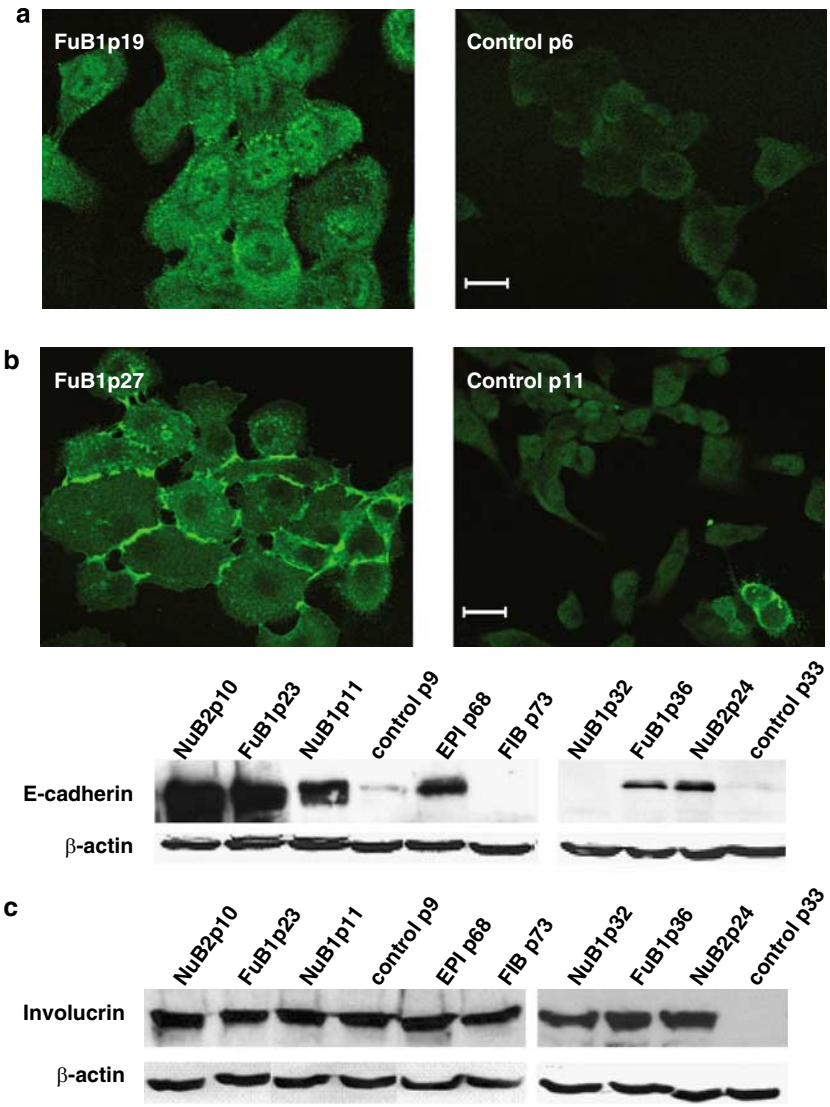

Figure 4. Characterization of desmoplakins and E-cadherin expression of Nox1 and control lines. (**a**) Using IIF, desmoplakins 1 and 2 were detected showing spotted staining at the cell-to-cell borders of FuB1p19 (left panel). No staining was found in control p6 (right panel). (**b**) Using IIF, E-cadherin was detected at the interjunctions of all Nox1 lines as shown for FuB1p27 (left panel). A few cells were positive for E-cadherin in control p11 (right panel). Using Western blot analysis, E-cadherin was detected in Nox1 lines and was very weakly present in control p9 and p33. (**c**) Involucrin protein was detected in all cell types at early passages. While involucrin of Nox1 lines was persistent at high passages, involucrin was completely absent in control p33. Bar = 50 μm.

comparison with other cobblestone Nox1 lines. Because IF type III vimentin is associated with epithelial–mesenchymal transition, we analyzed vimentin in Nox1 and control lines. Vimentin was evenly stained in the cytoplasm of every NuB1p8 cell and some cells showed strong focal vimentin staining (Figure 5a, left panel). Pronounced focal vimentin staining was observed in every NuB1p19 and NuB1p27 cell (not shown). Focal vimentin staining in the cytoplasm was also observed in 20% of FuB1p19 cells (Figure 5a, middle panel). Vimentin staining was faint in slowly proliferating control p6 (Figure 5a, right panel) and completely absent in fast proliferating control p27 (Table 1) (not shown). By using IIF, pan-keratins were strongly expressed in FuB1p19 but weaker in NuB1p8 and control p6 (not shown).

Keratin IF are heteropolymers of type I (K9–K19) and type II (K1–K8) polypeptides that constitute the bulk of the epithelial cytoskeleton. Among simple epithelial keratins, which are implicated with cell transformation (Diaz-Guerra *et al.*, 1992; Bisgaard *et al.*, 1994), keratin 18 (type I) forms a heterotypic coiled-coil complex with its natural partner keratin 8 (type II). We next investigated expression of K8 and K18 in control and Nox1 lines. With IIF using anti-K18 antibody (clone DC10 denoted as ab1) (Dianova, Hamburg, Germany) , K18 was stained in every cell of NuB1p14, FuB1p27, and NuB2p16 but only a few cells of control p11 (not shown). In Western blot analysis, ab1, although specific for K18, was immunoreactive with two proteins at 45 and 52 kDa for K18 and K8, respectively (Figure 5b). K18 was present in NuB1 p11 and

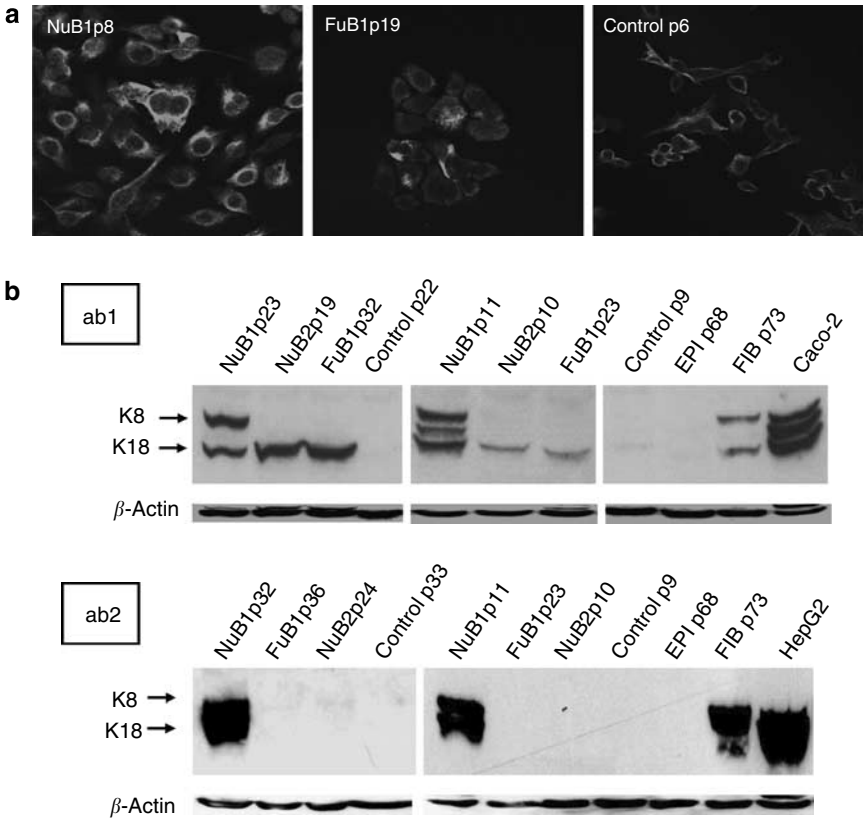

Figure 5. Expression of vimentin and simple epithelial keratin K8/K18 in Nox1 and control lines. (**a**) Using IIF, vimentin staining was detected in spindle-shaped NuB1p8 cells (left panel) and in ~20% of cobblestone FuB1p19 cells (middle panel). Control p6 showed faint vimentin staining (right panel). (**b**) Using Western blot analysis, expression of K8/K18 in Nox1 and control lines were compared using two types of antibodies from Dianova monoclonal K-18 antibody (ab1) and ICN monoclonal K8/K18 antibody (ab2). FIB, Caco-2, and HepG2 were (+) controls.

23, NuB2 p10 and 19, and FuB1 p23 and 32, FIB as well as Caco-2 cells. K18 levels appeared to increase upon passaging. K8 was present in NuB1 p11 and 23, FIB, and Caco-2 cells. An unknown ~50-kDa protein was present in NuB1p11 and Caco-2 cells. NuB1 shared similarity with Caco-2 in terms of K8/K18 expression. Neither K8 nor K18 was present in control p9 and 22 and EPI cells. From these data, ab1 appeared to be reactive with the individual K18 polypeptide as well as with the heteropolymeric K8/K18 complex.

Another mAb against both K8 and K18 from ICN (clone NCL 503 denoted as ab2) was used to confirm data using ab1. Ab2 detected K8 and K18 in NuB1 p11 and 32, FIB, and HepG2 cells (Figure 5b). Ab2 did not detect any K8/K18 in FuB1 p23 and 36, NuB2 p10 and 24, control p9 and 33, and EPI cells. Our observations here for K8/K18 by both ab1 and ab2 in EPI and FIB cells were consistent with our previous IIF data (Chamulitrat *et al.*, 2003a). Consistently, both ab1 and ab2 detected K8 and K18 in NuB1 but not in control cells. There was, however, a discrepancy in the lack of K18 detection in FuB1 and NuB2 lines when using ab2. While ab1 was a monoclonal antibody specific for K18, ab2 was specific for both K8 and K18. Ab2 may have been unreactive with (denatured or renatured) individual polypeptides, but could have reacted strongly with the heterotypic complex of K8/K18. This was previously studied and discussed for a monoclonal antibody against human K18 (Franke *et al.*, 1987). Taken together, the presence of K8 and K18 in Nox1 lines, especially NuB1, suggests an association of Nox1 with preneoplastic characters.

DISCUSSION

We demonstrated that Nox1-transfected cells undergoing rounds of confluence exhibited resistance against terminal differentiation to produce Nox1 lines. Nox1 lines were stable epithelial phenotypes and differentially expressed IF vimentin and K8/K18, whereas the control line did not. Our data demonstrate that Nox1 accelerated neoplastic progression by generating differentiation-resistant cells with indefinite lifespans in DMEM/FCS, and these cells, particularly in the NuB1 line, expressed neoplastic-like markers vimentin and K8/K18.

Tumorigenicity may result not only from mutation *per se* but also from clonal selection for resistance to a number of antiproliferative conditions that lead to neoplastic progression (Blagosklonny, 2002). Carcinogens and oncogenes may not always be cytotoxic but rather may be cytostatic by rendering resistance against Ca^{2+}/serum-induced terminal differentiation. If Nox1 represents an oncogene contributing to an early progression step, it is plausible that Nox1 elicits cytostatic effect by inducing resistance in an antiproliferative

condition. As summarized in Figure 6, we utilized immortal human keratinocytes to investigate multistep molecular events to include Nox1 overexpression and selection of preneoplastic cells using three to five rounds of confluence followed by exposure to differentiation inducer DMEM/FCS. Differentiation-resistant cells were immediately obtained in Nox1-transfected cells, resulting in five Nox1 lines. Without rounds of confluence, Nox1 transfections did not produce any resistant cells; thus, prolonged confluence plays a role in clonal selection of Nox1-dependent transformants. Without Nox1, it was very difficult to obtain a control line, indicating that Nox1 accelerated the selection process. Consistently, a carcinogen or stress benzo[*a*]pyrene (Zhu and Gooderham, 2002), or hypoxia (Kim *et al.*, 1997 (Karen *et al.*, 1999), Nox1 lines may harbor a genetic lesion in the first step. The second step leads to clonal expansion of these initiated cells under selective conditions, that is, confluence rounds and DMEM/FCS exposure. Our ability to obtain Nox1 lines in a reproducible manner suggests the important role of epigenetic influence on selection and expansion of potentially premalignant cells initiated by Nox1.

Nox1-derived ROS may elicit cytostatic consequences by mediating MAP kinases as proliferative signals (Gupta *et al.*, 1999). ROS may interfere with cell cycle machinery as supported by data showing oxidant-induced inactivation of mitotic inhibitor $p16^{INK4a}$ by hypermethylation (Govindarajan *et al.*, 2002) and destruction of $p16^{INK4a}$–cdk4 interaction (Martin *et al.*, 2000). Recent data show that trace amounts of H_2O_2 (20–60 μM) can increase the cellular lifespans of human keratinocytes, with slowdown of age-dependent telomeric DNA shortening (Yokoo *et al.*, 2004). This is in accordance with our results for an immediate generation of oxidant-generating Nox1 lines; many attempted control cells had limited lifespans, and essentially died. It has been shown that adding H_2O_2 at 500 μM for 3 h mediates cellular senescence (Haendeler *et al.*, 2003). ROS generated from Nox1 under our conditions was at very low levels capable of mediating cellular longevity rather than senescence. In line with this, Nox-based components and ROS generation were increased in Nox1 lines (i.e., immediate/reproducible generation) compared with control line (i.e., rare generation) (Figure 6).

Nox1 accelerated the generation of cells with indefinite lifespans in DMEM/FCS (Figure 6). An acquisition of indefinite lifespan or ''conversion'' has been previously described during viral oncogene overexpression of conditionally (slow growing) immortal cells (Garbe *et al.*, 1999). Although we observed fast-dividing cells when they first appeared after 7–10 days of DMEM exposure (Figure 2a), our Nox1 lines had different phenotypes after the first passage. This is in accordance with the notion that colony-forming human keratinocytes in culture can be of heterogeneous morphology with different growth potentials (Barrandon and Green, 1987). NuB1 appeared to contain a mixture of cells at a transitional stage with negative growth at low passages $P<15$, and as they reached a stable phenotype expressing increased Nox1 and resuming increased proliferation

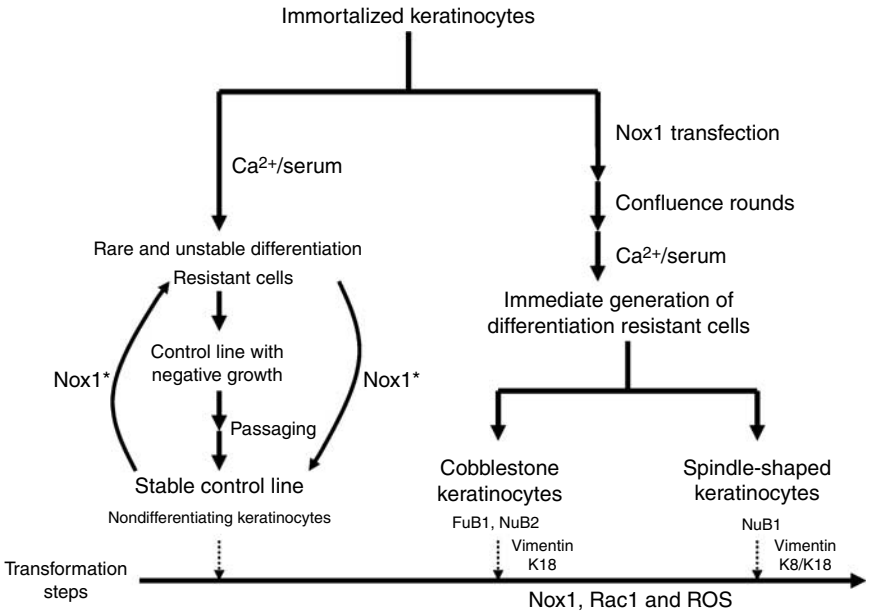

Figure 6. Schematic outlines for the role of Nox1 in induction of resistance against Ca^{2+}/serum-induced differentiation. Human keratinocytes immortalized with E6/E7 oncogenes of HPV16 were transfected with Nox1 and cultured in KGM with at least three rounds of confluence followed by exposure to DMEM/FCS. Nox1-transfection could overcome differentiation-induced cell death producing Nox1 lines. A control line was established from untransfected GM16 cells with initial negative growth. After prolonged culture in DMEM/FCS to $p>20$, these cells became stable growing, with the same growth rates as Nox1 lines. Stable control line expressed Nox1 protein at slightly lower than 63 kDa (denoted as Nox1*), indicating Nox1 induction during selection. All Nox1 lines showed increased Nox-based components and ROS generation compared with the control line. In contrast to the control line, Nox1 lines expressed involucrin, vimentin, and K8/K18, thus placing the control line at the lowest transformation steps. Increased vimentin and K8/K18 expression in spindle-shaped NuB1 compared with cobblestone Nox1 lines indicates that NuB1 is at higher transformation steps.

capacity (Table 1; Figure 3). This initial slow growth characteristic may be associated with phenotypic changes toward neoplastic progression as previously discussed for transformation of NIH3T3 (Chow and Rubin, 1999).

Similar to the NuB1 line, our control line had initially slow growth and proliferation increased at the same rates as Nox1 lines at $p > 22$. We found a protein slightly lower than 63-kDa by ~3 kDa. For rat Nox1 (Mitsushita *et al.*, 2004), it was speculated that the 3-kDa doublet structure could be due to post-translational degradation of Nox1. Nox1 was increased in control cells with increased passages to stable phenotype indicating an autocrine induction of smaller size Nox1 (denoted as Nox1*) after prolonged passaging in DMEM/FCS (Figure 6). Nox1* and growth-factor dependence were likely necessary for proliferation of the control line. In line with this, it has been shown that EGF stimulation to generate H_2O_2 is mediated by Nox1 (Park *et al.*, 2004). This control line, although polygonal-shaped, differed significantly from NuB1. The E6/E7 oncogene of HPV16, used to immortalize GM16 cells, was likely responsible for differentiation resistance to generate the control line (Sherman and Schlegel, 1996). HPV18-immortalized cells could be adapted to growth in serum and high Ca^{2+} (Woodworth *et al.*, 1988), and some adapted cells can exhibit spindle-shaped morphology (Sashiyama *et al.*, 2002). Extended propagation (~p125) of DMEM-adapted HPV18-immortalized cells did not result in malignant progression (Woodworth *et al.*, 1988). This may be the case for our control line. The control line lacked expression of E-cadherin and involucrin; thus, they were classified as non-differentiating keratinoytes. The control line, however, expressed protein(s) with smaller-sized Nox1* and expressed lower levels of Rac1 protein and NOXO1 mRNA. The control line, thus generating lesser ROS, could be considered as less transformed compared with Nox1 lines (Figure 6).

ROS from Nox including Nox1 have been shown to regulate cell growth, and inhibition of Nox1 (Teshima *et al.*, 1998, Rokutan *et al.*, 2006) or Nox4 (Mochizuki *et al.*, 2006) induces apoptosis. Thus, Nox1-derived ROS may likely be cytostatic, mediating proliferative signals in cancer cells (Arbiser *et al.*, 2002), and partially transformed EPI, FIB, and HaCaT cells (Chamulitrat *et al.*, 2003b, 2004). Conversely, Nox1-derived ROS may increase transformation steps by increasing resistance against differentiation-induced cell death or apoptosis (Figure 6). Similar to keratinocytes such as HaCaT, Nox1 lines were stable epithelial phenotypes expressing epithelial markers E-cadherin, desmoplakins 1 and 2, and involucrin. Similar to HaCaT, FuB1 and NuB2 cells expressed 63-kDa Nox1 (Figure 3b), while NuB1 cells expressed both 63-kDa Nox1 and a protein slightly lower than 63 kDa-Nox1, which was also present in the control line. Although the significance of protein(s) at slightly lower than 63 kDa Nox1 (Nox1*) in the control and NuB1 cells is not yet known, one may speculate about an association with their fibroblast-like structure. Compared with the control line, all Nox1 lines generated increased ROS with concomitant increased Rac1 expression (Figure 3c and d); thus, Rac1 may be the determinant protein for regulating Nox1 activity in our Nox1 lines. This speculation is consistent with recent reports (Kawahara *et al.*, 2004; Cheng *et al.*, 2006; Miyano *et al.*, 2006). As all Nox1 lines (but not control) expressed terminal differentiation involucrin, Nox1 may play a role in differentiation of cancer cells as previously discussed (Geiszt *et al.*, 2003; Fukuyama *et al.*, 2005). While p47phox, p67phox, and NOXA1 mRNA were present in control and Nox1 lines, NOXO1 mRNA was detected only in NuB1, indicating that p47phox may have been substituted for NOXO1 for full Nox1 function in FuB1 and NuB2 lines.

Here, Nox1 overexpression not only accelerated selection process but also unequivocally produced neoplastic phenotypes that expressed simple epithelial keratin K18 or K8/K18. Exposure of mouse keratinocytes to 200 μM H_2O_2 for 2–4 days caused a conversion from epithelium to elongated phenotype together with induction of matrix metalloproteinase-2,-9, and -13, indicating invasive properties (Mori *et al.*, 2004). Matrix metalloproteinase-9 and K8/K18 (Chu *et al.*, 1997; Bisgaard *et al.*, 1994), as well as vimentin (Chu *et al.*, 1996), are associated with more invasive and metastasis properties of cancer cells. K8 is considered a marker of malignant progression in cancer cells (Diaz-Guerra *et al.*, 1992) and in vivo (Casanova *et al.*, 2004). The NuB1 line showed a loss of cell–cell adhesion molecule E-cadherin, with a switch from an epithelial cytokeratin to a mesenchymal vimentin IF phenotype. Spindle-shaped NuB1 cells undergoing epithelial–mesenchymal transition expressing persistent vimentin and K8 may likely be of an invasive phenotype. Similar to cobblestone Nox1 lines, HaCaT cells express both Nox1 (Chamulitrat *et al.*, 2004) and K18 (Caulin *et al.*, 1993). This bolsters the notion that cobblestone Nox1 lines such as FuB1 and NuB2 (expressing weak vimentin and K18) were non-malignant phenotypes with more transformation steps than control cell line (Figure 6). Spindle-shaped NuB1 expressing strong vimentin and K8/K18 may likely be more transformed than cobblestone Nox1 lines.

In conclusion, we provide evidence that Nox1 overexpression of immortalized human keratinocytes accelerated resistance to signals for terminal differentiation, generating progenitor cell lines, which at varying degrees expressed vimentin and K8/K18. These distinct alterations may likely be related to progressive changes during the early stage of epithelial neoplastic progression. In a multistep process, these progenitor cells may potentially progress further into more malignant states. Nox1 was effective in overcoming the differentiation block, with an acquisition of indefinite lifespan cells. This raises the possibility that Nox1 may affect the rate-limiting steps of human epithelial carcinogenesis.

MATERIALS AND METHODS

Cell culture

GM16 cells were grown in Clonetics KGM supplemented with singlequots from Cell Systems (St Katharinen, Germany). EPI and FIB cells cultured in DMEM (Sigma, Deisenhofen, Germany) containing 10% FCS (DMEM/FCS) were cell lines generated in our laboratory (Chamulitrat *et al.*, 2003a). FIB cells were more transformed than EPI cells by exhibiting AIG (Chamulitrat *et al.*, 2003b).

Preparation of Nox1 plasmids

Nox1 cDNAs were prepared from HT29 total RNA using Nox1-specific primers (Chamulitrat *et al.*, 2003b). DNA fragments of human Nox1 (between nucleotides 205–1838; GenBank accession # NM_007052) were amplified by reverse transcription–PCR using primers 5′-AAATTTAAGCTT ACCTCTTGACAATGGGAAACTGGG-3′ and 5′-AAATTTGATATCGAGACAAAATGCAGATTACCGTCC-3′ that contain *Hin*dIII and *Eco*RV sites (underlined, respectively). The Nox1 cDNA fragment was gel-purified and cloned into pcDNA3.1/NT-GFP-TOPO using the NT-GFP fusion TOPO-TA kit (Invitrogen, Karlsruhe, Germany), and further subcloned into pcDNA3.1. The correct molecular size of pcDNA3.1/Nox1 was confirmed by DNA sequencing. Linearized plasmids cut with *Sca*I were used to generate resistant Nox1 lines. Supercoiled plasmids were used for transient transfection.

Determination of ROS in transfected GM16 cells

Hydroethidine is a fluorescent probe reported to be specific for superoxide radicals (Benov *et al.*, 1998). At 24 hours post transfection, cells were treated with 10 μM hydroethidine (Molecular Probes, Leiden, Netherlands) for 20 minutes at 37°C. After washing with phosphate-buffered saline (PBS), treated cells were examined with an Olympus IX50 microscope. For each transfection, cells showing oxidized hydroethidine as red fluorescence in cytoplasm were counted from six fields with 100–200 cells per field.

Transfection and selection of transfected GM16 cells

The sequence of the procedure is shown in Figure 1a. GM16 cells p34 (0.5×10^6 cells seeded in KGM in each well of six-well plates 24 hours earlier) were subjected to two methods of transfection using the human keratinocyte Nucleofector™ kit for adult human keratinocytes using the T24 program (Amaxa GmbH, Köln, Germany) or Fugene6 (Roche Diagnostics, Mannheim, Germany). After 24 hours, the transfection medium was replaced by KGM containing 0.8 mg/ml G418. At 48 hours post transfection, cells were transferred to T25 Falcon flasks and cultured without trypsinization for 4 weeks, with a change of KGM containing G418 every week. Cells were trypsinized and transferred to T75 flasks and cultured without trypsinization further for 4 weeks in KGM containing G418. At this point, Batch1 was initiated, where confluent cells were trypsinized and split into three portions; one half was seeded in a T75 for NuB1 and in a T25 for FuB1 in KGM (which was replaced with DMEM/FCS 24 hours later for selection), a quarter was for Western blot analysis of Nox1, and the remaining quarter was seeded in a T75 for subcultures in KGM in the absence of G418. The latter portion of cells were grown to confluence and trypsinized (designated as Batch2) with a 1:2 split ratio for selection in DMEM/FCS in a T25 and for subculture in KGM in a T75, respectively. This process was repeated for Batch3; 1:2 split cells were either frozen or exposed to DMEM/FCS for selection in a T25. The selection process was performed by culturing cells in DMEM/FCS for 2–3 weeks without trypsinization according to a reported protocol (Schlegel *et al.*, 1988). Terminally differentiated dead cells were removed by a change of medium every 2–3 days. Cells were regularly inspected under a phase-contrast microscope to identify for an outgrowth of resistant cells. Five resistant cells termed as ''Nox1 lines'' were obtained. Nox1 lines were passaged in DMEM/FCS at 1:2 every 3–4 days.

To determine the significance of confluence rounds, we performed two sets of Fugene6 transfection of GM16 cells with pcDNA3.1 or pcDNA3.1/Nox1. Transfected cells were exposed to DMEM/FCS containing G418 48 hours later without allowing them to undergo confluence rounds. One resistant cell population (noted as FT cells for failed transfection in Figure 3a) was obtained and subjected to Nox1 protein analysis. These cells were proliferative up to only p14 and then died. Several attempts were carried out using untransfected GM16 cells. One attempt was to culture untransfected GM16 cells in KGM in the same manner as described in Figure 1a, and this failed. Three other attempts were to directly expose untransfected GM16 cells (p34) to DMEM/FCS. In general, single elongated or flattened cells were first observed at 6–10 weeks in DMEM/FCS but failed to maintain proliferation. Only one resistant population was obtained after 6 weeks of DMEM/FCS exposure; it grew very slowly at a 1:2 split every 3 weeks. Upon passaging, these cells gained proliferation at $p > 20$ at the same rates as Nox1 lines. These cells were regarded as the control line.

Growth characteristics

Growth characteristics were determined as PD and AIG. For the PD study, 3×10^5 cells were seeded in a 100-mm dish. Medium was changed every 2–3 days before high density could slow down their growth. PD per day was determined from $PD = \log_2$ (number of cells at the time of harvest)/(number of cells seeded) divided by number of days in culture (Dickson *et al.*, 2000). AIG of NuB1p22, FuB1p31, NuB2p18, and control p21 was assayed to determine the ability to proliferate on semi-solid agar using standard procedures (Chamulitrat *et al.*, 2003a).

Determination of ROS in Nox1 and control lines

Nox1 and control lines (1×10^6 cells) were seeded in each well of six-well plates overnight. Cells were incubated in PBS for 15 min before trysinization. Cells were washed with PBS twice and resuspended in 1 ml serum-free DMEM. ROS generation was determined following the addition of dichlorofluorescein diacetate (Molecular Probes) at 5 μM final concentration to 300 μl cells. After a 10-min incubation, green fluorescence (FL1) generated by 10,000 cells was measured with a BD FACSCalibur™ flow cytometer. Effects of EGF were studied by adding EGF (100 ng/ml) for 10 min prior to dichlorofluorescein diacetate addition. Alternative quantitative ROS generation was performed using the cellular luminescence enhancement system for superoxide detection (Diogenes™, National Diagnostics, Atlanta, GA). Cells were washed and resuspended in PBS containing 5 mM glucose, 1 mM $MgCl_2$, and 0.5 mM $CaCl_2$. Luminescence from 5×10^5 cells in 150 μl PBS was measured at room temperature using a luminometer (Auto Lumat LB953, EG&G Berthold). Luminescence as a measure of superoxide radical was tested with the use of superoxide dismutase (3 μg/ml) to inhibit luminescence. ROS determination by both techniques was reproducible from three cell preparations with at least four determinations for each cell type.

Reverse transcription–PCR of Nox-based components

Total RNA was prepared from Nox1 and control lines. Reverse transcription was performed using Nox1 gene-specific-priming and PCR amplification of Nox1 mRNA was performed (Chamulitrat *et al.*, 2003b). PCR amplifications of polydT-primed reverse transcription were carried out using reported primers for p22*phox*, p47*phox*, p67*phox*, NOXO1 (Kawahara *et al.*, 2004), and NOXA1 (Ueno *et al.*, 2005).

Western blot analyses

To make polyclonal anti-Nox1 antibody, a polypeptide of 13 amino acids of human Nox1 C-terminus (at 544–556, CHRYSSLDPRKVQ) was synthesized at the German Cancer Research Center, Heidelberg. Immunization of rabbits and affinity purification was performed by Biotrend Chemikalien GmbH, Cologne, Germany. For Western blot analysis, our Nox1 antibody was tested against Nox1C2 antibody (a kind gift from Professor Rokutan). Our Nox1 antibody could detect Nox1 protein at 63 kDa; however, it also strongly detected 55- and 45-kDa proteins. For Western blot analysis of Nox1, membranes were prepared as previously described (Chamulitrat *et al*., 2003b). In some preparations, membrane was solubilized with 4 M urea to produce a homogeneous membrane sample. In each lane, 10 μg membrane proteins (from $\sim$1 to 3×10^6 cells) of transfected GM16 cells (Batch1) and 50 µg membrane proteins (from $\sim 30 \times 10^6$ cells) of Nox1 and control lines were subjected to electrophoresis and then electrotransferred. The blots were incubated with 1:1000 anti-Nox1 antibody overnight at 4°C.

For Western blot analysis of other proteins, cell lysates (25 or 50 μg proteins per lane) prepared from Nox1 and control lines were separated and electrotransferred onto membranes. Blots were incubated with 1:1000 anti-Rac1 (BD transduction, Heidelberg, Germany), 1:2500 anti-E-cadherin (clone 36, BD transduction), 1:500 anti-K18 (ab-1 clone DC10, Dianova, Hamburg, Germany), 1:1000 involucrin (clone SY5, Sigma), or 1:500 anti-K8/K18 (clone NCL503, ICN, OH) overnight at 4°C. The blots were incubated with a secondary anti-mouse or anti-rabbit antibody. Blots were stripped and reprobed with β-actin antibody.

Indirect immunofluorescence

Cells were fixed and stained with 1:200 anti-vimentin antibody (Monosan, Uden, The Netherlands), pan-keratin (Lu-5, Dianova), desmoplakins 1 and 2 (gifts from W. Franke, German Cancer Center, Heidelberg), E-cadherin (BD transduction), or K18 (ab-1, Dianova) as previously performed (Chamulitrat *et al*. 2003a).

CONFLICT OF INTEREST

The authors state no conflict of interest.

ACKNOWLEDGMENTS

We thank Dr. R. Schmidt for technical advice on cloning techniques, Dr. P. Tomakidi and Professor W. Franke for their generous gifts of antibodies, and K. Bents for sequencing of Nox1 plasmids. This study was supported by Deustche Forschungsgemeinschaft (CH 288/3-1).

REFERENCES

Adams JC, Watt FM (1988) An unusual strain of human keratinocytes which do not stratify or undergo terminal differentiation in culture. *J Cell Biol* 107:1927–38

Arbiser JL, Petros J, Klafter R, Govindajaran B, McLaughlin ER, Brown LF *et al.* (2002) Reactive oxygen generated by Nox1 triggers the angiogenic switch. *Proc Natl Acad Sci USA* 22:715–20

Barrandon Y, Green H (1987) Three clonal types of keratinocyte with different capacities for multiplication. *Proc Natl Acad Sci USA* 84:2302–6

Benov L, Sztejnberg L, Fridovich I (1998) Critical evaluation of the use of hydroethidine as a measure of superoxide anion radical. *Free Radic Biol Med* 25:826–31

Bisgaard HC, Ton PT, Nagy P, Thorgeirsson SS (1994) Phenotypic modulation of keratins, vimentin, and alpha-fetoprotein in cultured rat liver epithelial cells after chemical, oncogene, and spontaneous transformation. *J Cell Physiol* 159:485–94

Blagosklonny MV (2002) Oncogenic resistance to growth-limiting conditions. *Nat Rev Cancer* 2:221–5

Casanova ML, Bravo A, Martinez-Palacio J, Fernandez-Acenero MJ, Villanueva C, Larcher F *et al.* (2004) Epidermal abnormalities and increased malignancy of skin tumors in human epidermal keratin 8-expressing transgenic mice. *FASEB J* 18:1556–8

Caulin C, Bauluz C, Gandarillas A, Cano A, Quintanilla M (1993) Changes in keratin expression during malignant progression of transformed mouse epidermal keratinocytes. *Exp Cell Res* 204:11–21

Chamulitrat W, Schmidt R, Chunglok W, Tomakidi P (2003a) Epithelium-like and fibroblast-like phenotypes derived from HPV16 E6/E7-immortalized human gingival keratinocytes following chronic ethanol treatment. *Eur J Cell Biol* 82:313–22

Chamulitrat W, Schmidt R, Tomakidi P, Stremmel W, Chunglok W, Kawahara T *et al.* (2003b) Association of gp91*phox* homolog Nox1 with anchorage independent growth and MAP kinase-activation of transformed human keratinocytes. *Oncogene* 22:6045–53

Chamulitrat W, Stremmel W, Kawahara T, Rokutan K, Fujii H, Wingler K *et al.* (2004) A constitutive NADPH oxidase-like system containing gp91phox homologs in human keratinocytes. *J Invest Dermatol* 122:1000–9

Cheng G, Cao Z, Xu X, van Meir EG, Lambeth JD (2001) Homologs of gp91phox: cloning and tissue expression of Nox3, Nox4, and Nox5. *Gene* 269:131–40

Cheng G, Diebold BA, Hughes Y, Lambeth JD (2006) Nox1-dependent reactive oxygen generation is regulated by Rac1. *J Biol Chem* 281:17718–26

Chow M, Rubin H (1999) Relation of the slow growth phenotype to neoplastic transformation: possible significance for human cancer. *In vitro Cell Dev Biol Anim* 35:449–58

Chu YW, Seftor EA, Romer LH, Hendrix MJ (1996) Experimental coexpression of vimentin and keratin intermediate filaments in human melanoma cells augments motility. *Am J Pathol* 148:63–9

Chu YW, Yang PC, Yang SC, Shyu YC, Hendrix MJ, Wu R *et al.* (1997) Selection of invasive and metastatic subpopulations from a human lung adenocarcinoma cell line. *Am J Respir Cell Mol Biol* 17:353–60

Diaz-Guerra M, Haddow S, Bauluz C, Jorcano JL, Cano A, Balmain A *et al.* (1992) Expression of simple epithelial cytokeratins in mouse epidermal keratinocytes harboring Harvey ras gene alterations. *Cancer Res* 52:680–7

Dickson MA, Hahn WC, Ino Y, Ronfard V, Wu JY, Weinberg RA *et al.* (2000) Human keratinocytes that express hTERT and also bypass a p16(INK4a)-enforced mechanism that limits life span become immortal yet retain normal growth and differentiation characteristics. *Mol Cell Biol* 20:1436–47

Franke WW, Winter S, Schmid E, Sollner P, Hammerling G, Achtstatter T (1987) Monoclonal cytokeratin antibody recognizing a heterotypic complex: immunological probing of conformational states of cytoskeletal proteins in filaments and in solution. *Exp Cell Res* 173:17–37

Fukuyama M, Rokutan K, Sano T, Miyake H, Shimada M, Tashiro S (2005) Overexpression of a novel superoxide producing enzyme, NADPH oxidase 1, in adenoma and well differentiated adenocarcinoma of the human colon. *Cancer Letters* 221:97–104

Garbe J, Wong M, Wigington D, Yaswen P, Stampfer MR (1999) Viral oncogenes accelerate conversion to immortality of cultured conditionally immortal human mammary epithelial cells. *Oncogene* 18:2169–80

Geiszt M, Lekstrom K, Brenner S, Hewitt S, Dana R, Malech H *et al.* (2003) NAD(P)H oxidase 1, a product of differentiated colon epithelial cells, can partially replace glycoprotein 91phox in the regulated production of superoxide by phagocytes. *J Immunol* 170:299–306

Goldman R, Moshonov S, Zor U (1998) Generation of reactive oxygen species in a human keratinocyte cell line: role of calcium. *Arch Biochem Biophys* 350:10–8

Goldring MB (2004) Immortalization of human articular chondrocytes for generation of stable, differentiated cell lines. *Methods Mol Med* 100:23–36

Govindarajan B, Klafter R, Miller MS, Mansur C, Mizesko M, Bai X *et al.* (2002) Reactive oxygen-induced carcinogenesis causes hypermethylation of p16(Ink4a) and activation of MAP kinase. *Mol Med* 8:1–8

Gupta A, Rosenberger SF, Bowden GT (1999) Increased ROS levels contribute to elevated transcription factor and MAP kinase activities in malignantly progressed mouse keratinocyte cell lines. *Carcinogenesis* 20:2063–73

Haendeler J, Hoffmann J, Brandes RP, Zeiher AM, Dimmeler S (2003) Hydrogen peroxide triggers nuclear export of telomerase reverse transcriptase via Src kinase family-dependent phosphorylation of tyrosine 707. *Mol Cell Biol* 23:4598–610

Hilenski LL, Clempus RE, Quinn MT, Lambeth JD, Griendling KK (2004) Distinct subcellular localizations of Nox1 and Nox4 in vascular smooth muscle cells. *Arterioscler Thromb Vasc Biol* 24:677–83

Karen J, Wang Y, Javaherian A, Vaccariello M, Fusenig NE, Garlick JA (1999) 12-*o*-tetradecanoylphorbol-13-acetate induces clonal expansion of potentially malignant keratinocytes in a tissue model of early neoplastic progression. *Cancer Res* 59:474–81

Kawahara T, Kuwano Y, Teshima-Kondo S, Takeya R, Sumimoto H, Kishi K *et al.* (2004) Role of nicotinamide adenine dinucleotide phosphate oxidase 1 in oxidative burst response to Toll-like receptor 5 signaling in large intestinal epithelial cells. *J Immunol* 172:3051–8

Kim CY, Tsai MH, Osmanian C, Graeber TG, Lee JE, Giffard RG *et al.* (1997) Selection of human cervical epithelial cells that possess reduced apoptotic potential to low-oxygen conditions. *Cancer Res* 57:4200–4

Kulesz-Martin M, Kilkenny AE, Holbrook KA, Digernes V, Yuspa SH (1983) Properties of carcinogen altered mouse epidermal cells resistant to calcium-induced terminal differentiation. *Carcinogenesis* 4:1367–77

Kuwano Y, Kawahara T, Yamamoto H, Teshima-Kondo S, Tominaga K, Masuda K *et al.* (2006) Interferon-gamma activates transcription of NADPH oxidase 1 gene and upregulates production of superoxide anion by human large intestinal epithelial cells. *Am J Physiol Cell Physiol* 290:C433–43

Lassegue B, Sorescu D, Szocs K, Yin Q, Akers M, Zhang Y *et al.* (2001) Novel gp91(phox) homologues in vascular smooth muscle cells : nox1 mediates angiotensin II-induced superoxide formation and redox-sensitive signaling pathways. *Circ Res* 88:888–94

Lee LW, Tsao MS, Grisham JW, Smith GJ (1989) Emergence of neoplastic transformants spontaneously or after exposure to *N*-methyl-*N*′-nitro-*N*-nitrosoguanidine in populations of rat liver epithelial cells cultured under selective and nonselective conditions. *Am J Pathol* 135:63–71

Lim SD, Sun C, Lambeth JD, Marshall F, Amin M, Chung L *et al.* (2005) Increased Nox1 and hydrogen peroxide in prostate cancer. *Prostate* 62:200–7

Martin EA, Robinson PJ, Franklin RA (2000) Oxidative stress regulates the interaction of p16 with Cdk4. *Biochem Biophys Res Commun* 275:764–7

Mitsushita J, Lambeth JD, Kamata T (2004) The superoxide-generating oxidase Nox1 is functionally required for Ras oncogene transformation. *Cancer Res* 64:3580–5

Miyano K, Ueno N, Takeya R, Sumimoto H (2006) Direct involvement of the small GTPase Rac in activation of the superoxide-producing NADPH oxidase Nox1. *J Biol Chem* 281:21857–68

Mochizuki T, Furuta S, Mitsushita J, Shang WH, Ito M, Yokoo Y *et al.* (2006) Inhibition of NADPH oxidase 4 activates apoptosis via the AKT/apoptosis signal-regulating kinase 1 pathway in pancreatic cancer PANC-1 cells. *Oncogene* 25:3699–707

Mori K, Shibanuma M, Nose K (2004) Invasive potential induced under long-term oxidative stress in mammary epithelial cells. *Cancer Res* 64:7464–72

Park HS, Lee SH, Park D, Lee JS, Ryu SH, Lee WJ *et al.* (2004) Sequential activation of phosphatidylinositol 3-kinase, beta Pix, Rac1, and Nox1 in growth factor-induced production of H_2O_2. *Mol Cell Biol* 24:4384–94

Rheinwald JG, Beckett MA (1980) Defective terminal differentiation in culture as a consistent and selectable character of malignant human keratinocytes. *Cell* 22:629–32

Rokutan K, Kawahara T, Kuwano Y, Tominaga K, Sekiyama A, Teshima-Kondo S (2006) NADPH oxidases in the gastrointestinal tract: a potential role of Nox1 in innate immune response and carcinogenesis. *Antioxid Redox Signal* 8:1573–82

Rubin H (2001) Selected cell and selective microenvironment in neoplastic development. *Cancer Res* 61:799–807

Sashiyama H, Shino Y, Sakao S, Shimada H, Kobayashi S, Ochiai T *et al.* (2002) Alteration of integrin expression relates to malignant progression of human papillomavirus-immortalized esophageal keratinocytes. *Cancer Lett* 177:21–8

Schlegel R, Phelps WC, Zhang Y-L, Barbosa M (1988) Quantitative keratinocyte assay detects two biological activities of human papillomavirus DNA and identifies viral types associated with cervical carcinomas. *EMBO J* 7:3181–7

Sherman L, Schlegel R (1996) Serum- and calcium-induced differentiation of human keratinocytes is inhibited by the E6 oncoprotein of human papillomavirus type 16. *J Virol* 70:3269–79

Suh YA, Arnold RS, Lassegue B, Shi J, Xu X, Sorescu D *et al.* (1999) Cell transformation by the superoxide-generating oxidase Mox1. *Nature* 401:79–82

Teshima S, Rokutan K, Nikawa T, Kishi K (1998) Guinea pig gastric mucosal cells produce abundant superoxide anion through an NADPH oxidase-like system. *Gastroenterology* 115:1186–96

Ueno N, Takeya R, Miyano K, Kikuchi H, Sumimoto H (2005) The NADPH oxidase Nox3 constitutively produces superoxide in a p22phox-dependent manner: its regulation by oxidase organizers and activators. *J Biol Chem* 280:23328–39

Woodworth CD, Bowden PE, Doniger J, Pirisi L, Barnes W, Lancaster WD *et al.* (1988) Characterization of normal human exocervical epithelial cells immortalized *in vitro* by papillomavirus types 16 and 18 DNA. *Cancer Res* 48:4620–8

Yang D, Louden C, Reinhold DS, Kohler SK, Maher VM, McCormick JJ (1992) Malignant transformation of human fibroblast cell strain MSU-1.1 by (+-)-7 beta,8 alpha-dihydroxy-9 alpha,10 alpha-epoxy-7,8,9,10-tetrahydrobenzo[a]pyrene. *Proc Natl Acad Sci USA* 89:2237–41

Yang J-Q, Li S, Domann FE, Buettner GR, Oberley LW (1999) Superoxide generation in v-Ha-ras-transduced human keratinocyte HaCaT cells. *Mol Carcinogenesis* 26:180–8

Yokoo S, Furumoto K, Hiyama E, Miwa N (2004) Slow-down of age-dependent telomere shortening is executed in human skin keratinocytes by hormesis-like-effects of trace hydrogen peroxide or by anti-oxidative effects of pro-vitamin C in common concurrently with reduction of intracellular oxidative stress. *J Cell Biochem* 93:588–97

Zhao YL, Piao CQ, Wu LJ, Suzuki M, Hei TK (2000) Differentially expressed genes in asbestos-induced tumorigenic human bronchial epithelial cells: implication for mechanism. *Carcinogenesis* 21:2005–10

Zhu H, Gooderham N (2002) Neoplastic transformation of human lung fibroblast MRC-5 SV2 cells induced by benzo[a]pyrene and confluence culture. *Cancer Res* 62:4605–9